Effect of moisture transfer on thermal inertia in simple layer walls: case of a vegetal fibre material

C. Maalouf, A.D. Tran Le, M. Lachi, E. Wurtz, T.H. Mai

Abstract**—**In building design, thermal inertia is an important passive parameter that affects occupants' thermal comfort. The purpose of this paper is to study the effect of moisture transfer on material thermal inertia for different materials by studying the behaviour of a simple wall under variating outdoor conditions and mainly to study transient hygrothermal behaviour of a vegetal fibre material made of a mixture of lime and hemp fibres. To study moisture transfer in materials, we used a coupled heat and moisture transfer model in which moisture transport is made through liquid and vapour phases. The liquid phase is supposed to move by capillarity whereas the vapour phase diffuses under vapour partial pressure gradient. For the numerical approach, a simulation model was developed and implemented in the program oriented object SPARK. Simulations were used to study the effect of moisture transfer on the damping effect, time lag and heat conduction loads through simple layer walls.

Keywords**—**Heat and moisture transfer, hemp concrete, simulation, thermal inertia, SPARK.

NOMENCLATURE

Symbol	Definition	Unit
C	Specific heat	$J\ kg^{-1}.K^{-1}$
C_0	Specific heat of dry material	$J\ kg^{-1}.K^{-1}$
C_l	Specific heat of water	$J\ kg^{-1}.K^{-1}$
D_T	Mass transport coefficient associated to a temperature gradient	$m^2.s^{-1}.°C^{-1}$
$D_{T,v}$	Vapor transport coefficient associated to a temperature gradient	$m^2.s^{-1}.°C^{-1}$
D_θ	Mass transport coefficient associated to a moisture content gradient	$m^2.s^{-1}$
$D_{\theta v}$	Vapor transport coefficient associated to a moisture content gradient	$m^2.s^{-1}$
g	Gravity acceleration	$m^2.s^{-1}$
h_M	Mass transfer convection coefficient	$kg.m^{-2}.s^{-1}$
h_T	Heat transfer convection coefficient	$W.K^{-1}m^{-2}$
L_v	Heat of vaporization	$J.kg^{-1}$
T	Temperature	°C
t	Time	s
α	Solar radiation absorption coefficient	
θ	Moisture content	$m^3.m^{-3}$
λ	Thermal conductivity	$W.m^{-2}K^{-1}$
ρ_0	Mass density of dry material	$kg.m^{-3}$
ρ_l	Mass density of water	$kg.m^{-3}$
ρ_v	Mass density of vapor water	$kg.m^{-3}$

C. Maalouf, A.D. Tran Le, M. Lachi, T.H. Mai are with Laboratoire Thermomécanique- GRESPI, Faculté des Sciences, University of Reims, BP1039, 51687, Reims, France (Corresponding author: chadi.maalouf@univ-reims.fr).

E. Wurtz is with LOCIE FRE CNRS 3220, University of Savoy -73377, Le Bourget du Lac Cedex, France

I. INTRODUCTION

In France, about 44% of energy consumption and 25% of carbon dioxide emission are due to building sector [1]. In order to reduce energy consumption, big care should be given to building design and mainly its envelope because it is the main barrier that protects from the outside weather or other conditions, such as cold in the winter, heat in the summer, humidity, rain, wind and noise. This requires studying the interaction of building envelope with outdoor variating conditions which is a form of thermal inertia [2]: It considers envelope behaviour under periodical time varying meteorological conditions. This inertia causes two important effects on the heat between indoor and outdoor environment like on amplitude reduction of the indoor temperatures and time-lag of the same ones in relation to the outdoor temperatures [3]–[7].

The purpose of this paper is to study effect of moisture transfer on thermal inertia of simple layer walls: its effect on the amplitude reduction and the time lag. We consider three building construction materials: normal concrete, brick and hemp concrete. The interest of the latter material is due to its low environmental impact which can be seen through its grey energy which is 90 kWh/m^3 and it is lower than normal concrete and brick grey energy (430 kWh/m^3 and 696 kWh/m^3. respectively). It is an ecological building material [8].

First we present the equations of the coupled heat and mass transfer model (HAM). These equations were implemented in the simulation environment SPARK which is suited to complex problems [9]–[12]. Then we study the behaviour of a simple layer wall under outdoor variating summer conditions. Results are first shown when neglecting moisture transfer (Th model) and are then compared to the HAM model results for the three studied materials. More results are shown for the hemp concrete wall for different wall thicknesses and different initial volumic moisture content. A parametrical analysis is also done in order to identify physical parameters that affect wall behaviour. Finally wall behaviour is studied under real climatic conditions taking into account solar radiation for two French cities: Ajaccio and Carpentras.

In the next section we will present the model of the simple wall as it is implemented in SPARK, then we will present simulations.

II. PHYSICAL MODEL

We find in the literature several works concerning modeling the hygrothermal transfer. Most of the research is still carried out

by using phenomenological macroscopic models, introducing heuristic laws relating thermodynamic forces to fluxes through moisture and temperature dependent transport coefficient. In this way, one of the most used and accepted macroscopic models for studying heat and moisture transfer through porous material is the Phillip and de Vries model [13] which uses as driving potentials the temperature and moisture content gradient .While most studies on heat transport processes largely agree, no consensus in the choice of driving potentials for describing moisture transport phenomena exists at present and some authors modified the Phillip and de Vries model by using other driving potentials instead of the moisture content. We should cite Perdesen [14] who used the capillary pressure, but in practice it is difficult to be directly measured. Künzel [15] used the relative humidity as a potential. The calculation methodology employed by them is correct since it takes into account the discontinuity phenomenon at the interface.

However, in many circumstances, the direct use of the moisture content as the driving forces can be appropriate since it can be more computationally viable and, most of time moisture content is more useful parameter as it has a simple and direct physic meaning. Consequently, in this paper, we use the Umidus model [16] in which the moisture in porous material can be transported under liquid and vapour phases. The liquid phase is supposed to move by capillary pressure, while the vapor phase is supposed to be diffused due to partial pressure gradients. Considering these hypotheses, the governing moisture balance equation within the wall is given by

$$\frac{\partial \theta}{\partial \tau} = \frac{\partial}{\partial x}\left(D_T \frac{\partial T}{\partial x} \right) + \frac{\partial}{\partial x}\left(D_\theta \frac{\partial \theta}{\partial x} \right) \tag{1}$$

The boundary conditions for this equation are given by (x=0 and x=L):

$$-\rho_l \left(D_T \frac{\partial T}{\partial x} + D_\theta \frac{\partial \theta}{\partial x} \right)\Bigg|_{x=0,e} = h_{M,e}\left(\rho_{ve,a,e} - \rho_{ve,s,e} \right) \tag{2}$$

$$-\rho_l \left(D_T \frac{\partial T}{\partial x} + D_\theta \frac{\partial \theta}{\partial x} \right)\Bigg|_{x=L,i} = h_{M,i}\left(\rho_{ve,s,i} - \rho_{ve,a,i} \right) \tag{3}$$

The governing energy balance equation states that the temporal variation of energy is due to the net amount of heat received/lost by conduction and the phase change within pores:

$$\rho_0 Cp_m \frac{\partial T}{\partial \tau} = \frac{\partial}{\partial x}\left(\lambda_{app} \frac{\partial T}{\partial x} \right) + L_v \rho_l \left(\frac{\partial}{\partial x}\left(D_{T,v} \frac{\partial T}{\partial x} \right) + \frac{\partial}{\partial x}\left(D_{\theta,v} \frac{\partial \theta}{\partial x} \right) \right) \tag{4}$$

where

$$Cp_m = Cp_0 + Cp_l \frac{\rho_l}{\rho_0}\theta \tag{5}$$

And the boundary conditions for this equation are given by (x=0 and x=L):

$$-\lambda_{app}\frac{\partial T}{\partial x} - L_v \rho_l \left(D_{T,v}\frac{\partial T}{\partial x} + D_{\theta,v}\frac{\partial \theta}{\partial x} \right)\Bigg|_{x=0,e} = h_{T,e}\left(T_{a,e} - T_{s,e} \right) + L_v h_{M,e}\left(\rho_{ve,a,e} - \rho_{ve,s,e} \right) + \alpha_e \Phi_{ray,e} \tag{6}$$

$$-\lambda_{app}\frac{\partial T}{\partial x} - L_v \rho_l \left(D_{T,v}\frac{\partial T}{\partial x} + D_{\theta,v}\frac{\partial \theta}{\partial x} \right)\Bigg|_{x=L,i} = h_{T,i}\left(T_{s,i} - T_{a,i} \right) + L_v h_{M,i}\left(\rho_{ve,s,i} - \rho_{ve,a,i} \right) - \alpha_i \Phi_{ray,i} \tag{7}$$

III. NUMERICAL RESOLUTION, SIMULATION ENVIRONNEMENT SPARK AND VALIDATION

In order to solve the previous equation system, the numerical solution is based on the finite difference technique with an implicit scheme. For wall thicknesses less than 20 cm, the wall is discretized into 25 nodes and for higher thicknesses it is discretized into 50 nodes. For example, equation (1) can be written as:

$$\frac{\theta_j^{n+1} - \theta_j^n}{\Delta t} = \frac{1}{\Delta x}\left(D_T \frac{\partial T}{\partial x} + D_\theta \frac{\partial \theta}{\partial x} \right)_{j+1/2}^{n+1} - \frac{1}{\Delta x}\left(D_T \frac{\partial T}{\partial x} + D_\theta \frac{\partial \theta}{\partial x} \right)_{j-1/2}^{n+1} \tag{8}$$

Where the space and time steps are denoted respectively Δx and Δt and θ_j^n represents the scalar value θ of node j at the time n. Equation (8) can also be written as:

$$\frac{\theta_j^{n+1} - \theta_j^n}{\Delta t} = \frac{1}{\Delta x}\left(D_{T,j+1/2}^{n+1} \frac{T_{j+1}^{n+1} - T_j^{n+1}}{\Delta x} + D_{\theta,j+1/2}^{n+1} \frac{\theta_{j+1}^{n+1} - \theta_j^{n+1}}{\Delta x} \right) - \frac{1}{\Delta x}\left(D_{T,j-1/2}^{n+1} \frac{T_j^{n+1} - T_{j-1}^{n+1}}{\Delta x} + D_{\theta,j+1/2}^{n+1} \frac{\theta_j^{n+1} - \theta_{j-1}^{n+1}}{\Delta x} \right) \tag{9}$$

Which gives:

$$\left(\frac{\Delta x^2}{\Delta t} + D_{\theta,j+1/2}^{n+1} + D_{\theta,j-1/2}^{n+1} \right)\theta_j^{n+1} - D_{\theta,j+1/2}^{n+1}\theta_{j+1}^{n+1} - D_{\theta,j-1/2}^{n+1}\theta_{j-1}^{n+1} + \left(D_{T,j+1/2}^{n+1} + D_{T,j-1/2}^{n+1} \right)T_j^{n+1} - D_{T,j+1/2}^{n+1}T_{j+1}^{n+1} - D_{T,j-1/2}^{n+1}T_{j-1}^{n+1} = \theta_j^n \tag{10}$$

Details of system discretization are shown in [17]. Equations were implemented in the Simulation Problem Analysis and Research Kernel (SPARK), a simulation environment allowing to solve efficiently differential equation systems [9]-[12]. SPARK was developed by the Simulation Research Group at Lawrence Berkeley National Laboratory. Description of a

problem for SPARK solution begins by breaking it down in an object-oriented way. This means thinking about the problem in terms of its components. Each component is represented by a SPARK object that contains the mathematical model for the specific component. Since there may be several components of the same kind, SPARK object models, equations or group of equations, are defined in a generic manner called classes. Classes serve as templates for any number of objects required to formulate the whole problem. The problem model is then completed by linking objects together. Using graph theoretic techniques, SPARK reduces the size of the equation system and uses a Newton-Raphson iterative method to solve the reduced system and after convergence, solves for the remaining unknowns.

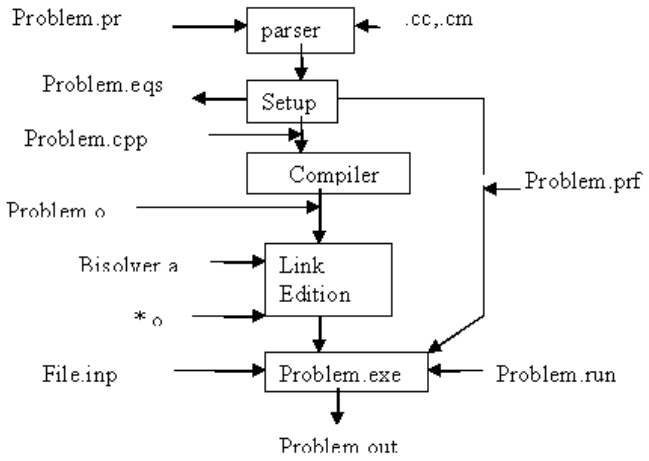

Fig. 1: Various stages for construction analyser in SPARK.

Figure 1 shows the various stages for construction analyser. The last one will be executed for a set of boundary conditions (and initial condition for a dynamic formulation). The boundary condition should be defined in the input files (files.inp) to solve solution for the problem (problem.out). The simulation parameters at the beginning, the end and the time step of the simulation are collected in the problem.run file. Resolution method as well as simulation performance (number of iterations …) are chosen in the problem.prf file.

The model presented in the last section was validated in the annex 41 of the International Energy Agency [18] and also by comparing numerical results with experimental results found in literature [19]. Details are found in [17] and [20]. In the following section, we will use this model to study the behaviour of a simple layer wall under outdoor variating conditions.

IV. STUDY OF A SIMPLE WALL SUBJECTED TO PERIODIC OUTDOOR CONDITIONS

In this section, we study the behaviour of a simple layer wall subjected to periodical outdoor temperature and relative humidity (Fig. 1). Indoor conditions are given as (for x=L): T_i=24°C; RH_i=50%; and $h_{T,i}$=5 W/m^{2}K where w=2*π/T and T= 24 hours. External outdoor conditions are given by sinusoidal functions and are shown in Fig. 2. External thermal convection coefficient is equal to $h_{T,e}$=25 W/m^{2}K . Indoor and outdoor mass transfer coefficients were calculated using the Lewis number relation for the air:

$$.Le = \frac{h_t}{h_m \rho C_p} = 1 \qquad (11)$$

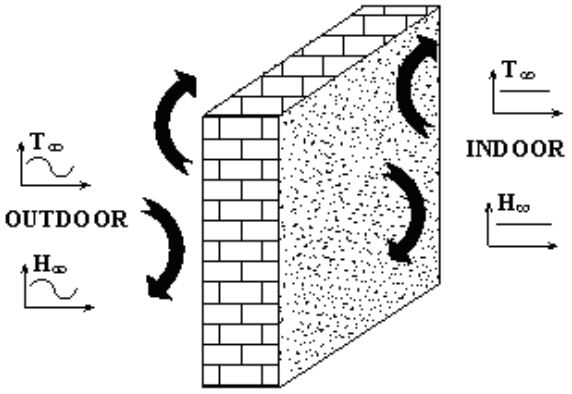

Fig. 2: Physical model for the simple layer wall.

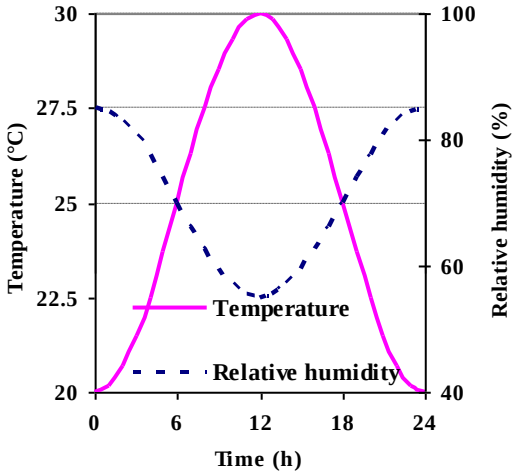

Fig. 3 : Sinusoidal functions for external temperature and relative humidity

The behaviour of three different materials used in construction was studied. These are: normal concrete, brick and hemp concrete. The input data (material properties, sorption isotherms, moisture diffusion coefficients) for normal concrete and brick were used from WUFI library [21]. Those for the hemp concrete are given in [22] and [23]. These data are shown in table 1. Material thermal properties (density, thermal conductivity and specific heat) are given for the dry material whereas moisture transport coefficients are for 50% relative humidity.

For the sorption isotherm curves they are shown in the Fig. 4.a. We have neglected hysteresis effect. We notice that for hemp concrete and brick, moisture diffusion coefficients are higher than normal concrete. Simulations were run for a period of 10 monthes, initial wall temperature was considered to be 20°C and the moisture content 0.0005 m^3/m^3 along the whole thickness. Wall thickness is 20 cm. For the three materials two cases were considered: the first one takes into account moisture

transfer through the material (HAM case) and the second one, neglects moisture transfer (Th case). For the Th case, dry

TABLE I:
MATERIAL PHYSICAL PROPERTIES

Material	Density	Thermal Conductivity	Specific heat	D_Θ	D_T	$D_{\Theta v}$	D_{Tv}
	kg/m3	*W/m.K*	*J/kg.K*	m^2/s	$m^2/(s.K)$	m^2/s	$m^2/(s.K)$
Normal concrete	2300	1.6	850	6.39E-10	7.91E-14	2.29E-11	7.91E-14
Brick	1630	0.6	850	1.1E-09	1E-11	1.1E-09	1E-11
Hemp concrete	413	0.1058	1000	1.16E-09	1.02E-12	1.07E-09	1.02E-12

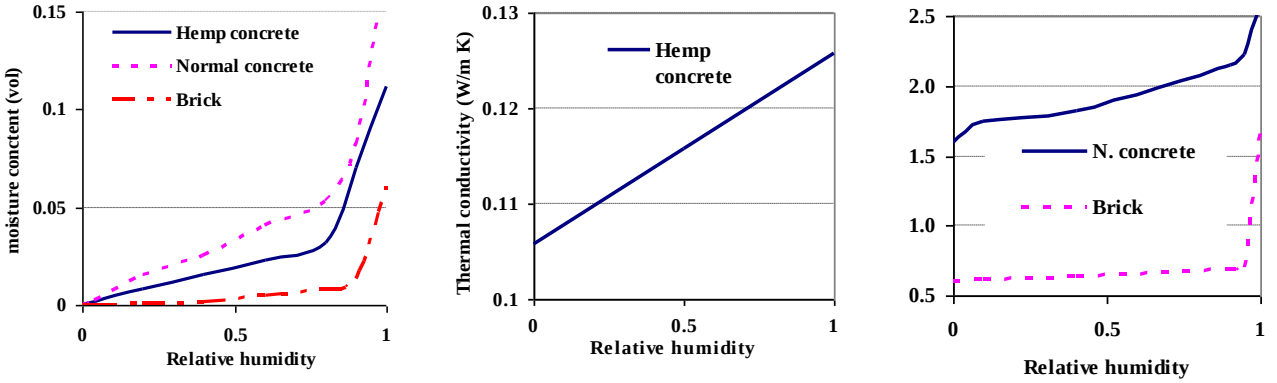

(a) (b) (c)

Fig. 4 : Sorption isotherms of the studied materials (a) and variation of their thermal conductivity with relative humidity (b and c).

material properties were used, transport and mass convection coefficients were set to 0. For the HAM case material thermal conductivity is a function of moisture content and it is shown in Fig. 4.b and 4.c.

V. RESULTS AND DISCUSSION

A. *For the Th model*

Fig. 5 shows time pattern of internal surface temperature for the three materials and for the heat transfer model (Th model). As shown in [2], this temperature, compared to outdoor temperature, is dampened and phase shifted. For the hemp concrete wall, temperature is the lowest and more dampened than other materials.

While outdoor temperature varies from 20°C to 30°C, internal surface temperature varies from 23.85°C to 24.34°C for the hemp concrete wall (Fig. 6). Therefore, the amplitude of the quasi-stationary mode is about 0.245°C while for a concrete wall it is about 1.43°C. The amplitude is being calculated as: $\theta = (T_{max} - T_{min})/ 2$. For the time lag, it also increases when thermal diffusivity decreases. It is determined graphically as shown in Fig. 5 for the hemp concrete where the outdoor temperature takes 7 hours to propagate to the inner surface.

Table II shows the thermal diffusivity, temperature amplitude, the mean internal surface temperature, time lag and heat conduction flux for the different studied materials. As the thermal diffusivity of the material increases, heat energy diffuses fastly within the wall, outdoor temperature propagates fastly (time lag is lower), temperature amplitude increases, the mean internal surface temperature becomes higher and heat conduction flux increases.

TABLE II: THERMAL DIFFUSIVITY, MEAN TEMPERATURE, AMPLITUDE OF THE QUASI-STATIONARY MODE, TIME LAG AND HEAT CONDUCTION FLUX THROUGH THE WALL.

Material	Thermal diffus. (m^2/s)	Mean T (°C)	Amp. of the stat. mode (°C)	Time lag (hour)	Max. conduction flux (W/m^2)	Min. conduction flux (W/m^2)
Concrete	8.18E-07	24.54	1.43	5.5	9.9	-4.42
Brick	4.33E-07	24.34	0.85	6.5	5.99	-2.5
Hemp concrete	2.55E-07	24.09	0.245	7	1.69	-0.75

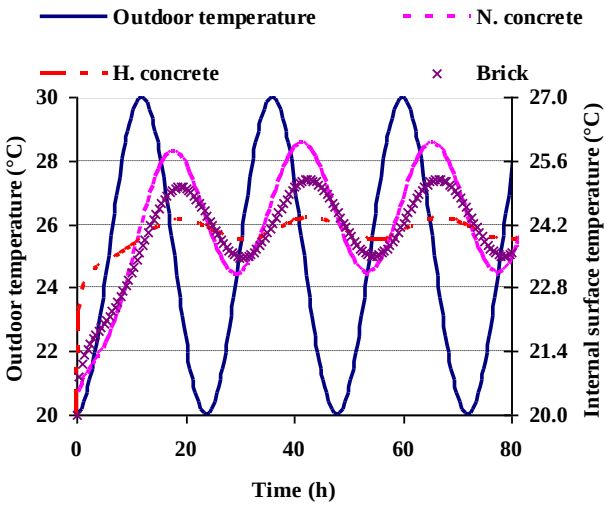

Fig. 5 : Time pattern of the wall internal surface temperature.

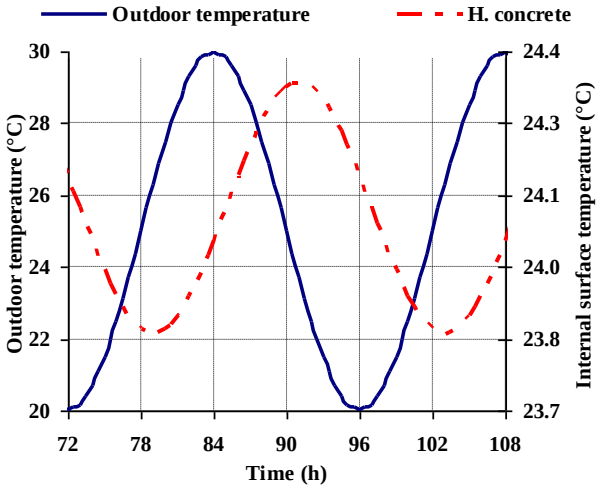

Fig. 6 : Time pattern of the hemp concrete wall internal surface temperature.

B. For the HAM model

Normal concrete wall

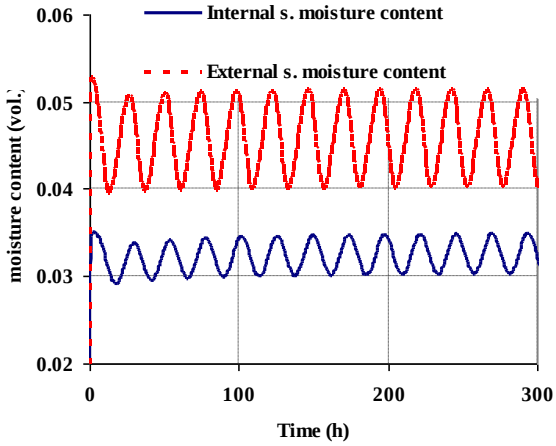

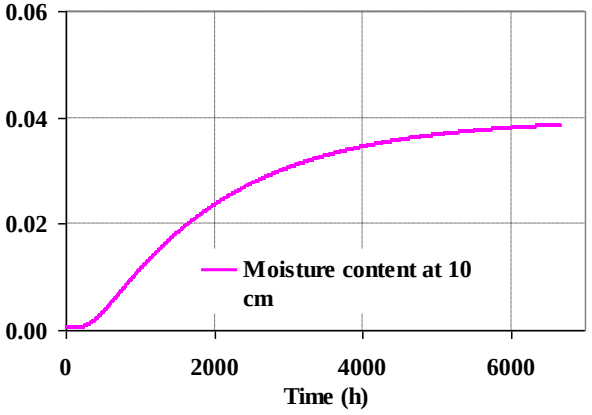

Fig. 7 : Variation of the moisture content on the external, internal surfaces and at a depth of 10 cm.

In this case taking into account moisture transfer through material leads to a growth in the thermal conductivity which will vary between 1.7 and 1.9 W/m K (depending on moisture content) instead of 1.6 in the Th model and also to an increase in the specific heat which will also vary between 905 and 941 J/kg K instead of 850 J/Kg K for the dry material. While moisture content on the internal and external surfaces reaches a periodical state in few days, it needs about six monthes to reach a steady state at a depth of 10cm inside the material (Fig. 7). However internal surface temperature profile sounds to vary very slightly after a period of one month. The amplitude of the HAM model is 1.36°C during the 10th day and there is no time lag between both model results (Fig. 8). When internal surface temperature is maximum, both model results are too close, the difference varies from 0.07°C on the 10th day to 0.02°C after one month and -0.01°C after 2.5 monthes. When temperature is minimum, the HAM model temperature is higher about 0.24°C on the 10th day, 0.18°C after one month and 0.13°C after 2.5 monthes. These differences are mainly due to the adsorption process when the temperature is minimum.

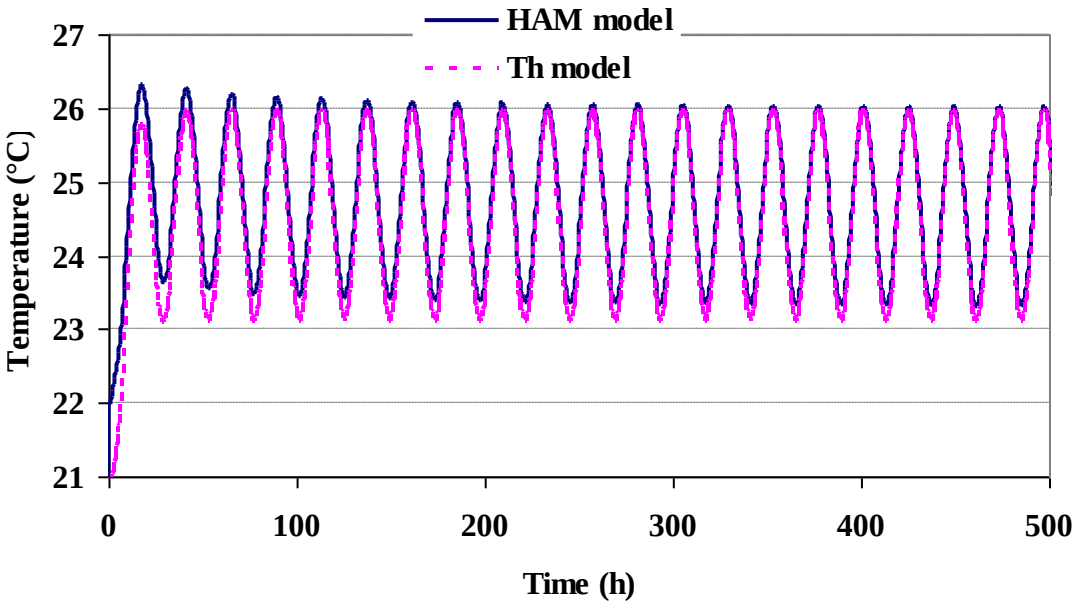

Fig. 8:Comparison between internal surface temperature patterns for both Th and HAM models for the concrete wall.

Brick wall

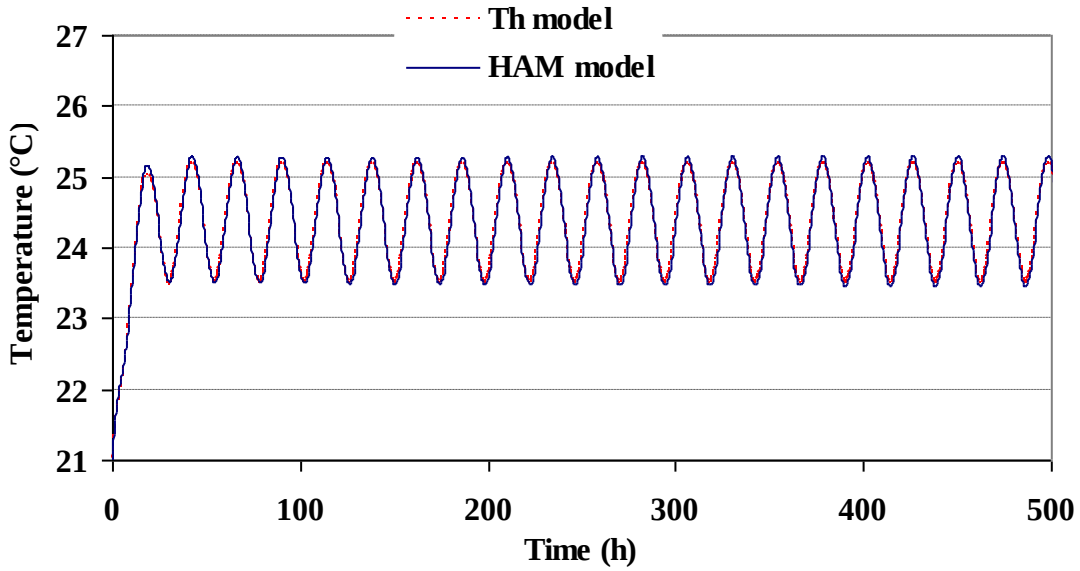

Fig. 9 : Comparison between internal surface temperature patterns for both Th and HAM models for the brick wall.

In this case taking into account moisture transfer through material has a very slight impact on the internal surface temperature (Fig. 9). When relative humidity varies between 55% and 85%, brick thermal conductivity varies between 0.65 to 0.68 W/m K in the HAM model instead of 0.6 in the Th model while the specific heat only increases from 850 to 860 J/Kg°C because brick moisture content is too low (it varies between 0.003 and 0.004 m^3/m^3). This means that thermal diffusivity increases leading to a slight increase in the internal surface amplitude. On the other side, because moisture transport coefficients are higher than concrete, moisture content inside the material varies slightly after only 3 monthes as shown in Fig. 10 and internal surface temperature changes are too small after only one month. On the tenth day, the internal surface temperature reaches 25.29°C in the HAM model compared to 25.2°C in the Th model. Considering the minimum value, HAM model result is lower of 0.015°C than that of the Th case. After one month, the difference reaches 0.11°C for the maximum value and 0.04°C for the minimum value. So the amplitude varies from 0.9°C on the 10^{th} day to 0.93°C after one month compared to 0.85°C for the Th model. The Th model temperature is also shifted of 15 minutes from the HAM model (the time lag of the HAM model gets lower). These results are only valid for values of outdoor relative humidity lower than 95% since brick thermal conductivity increases drastically for higher values because of its micro pores

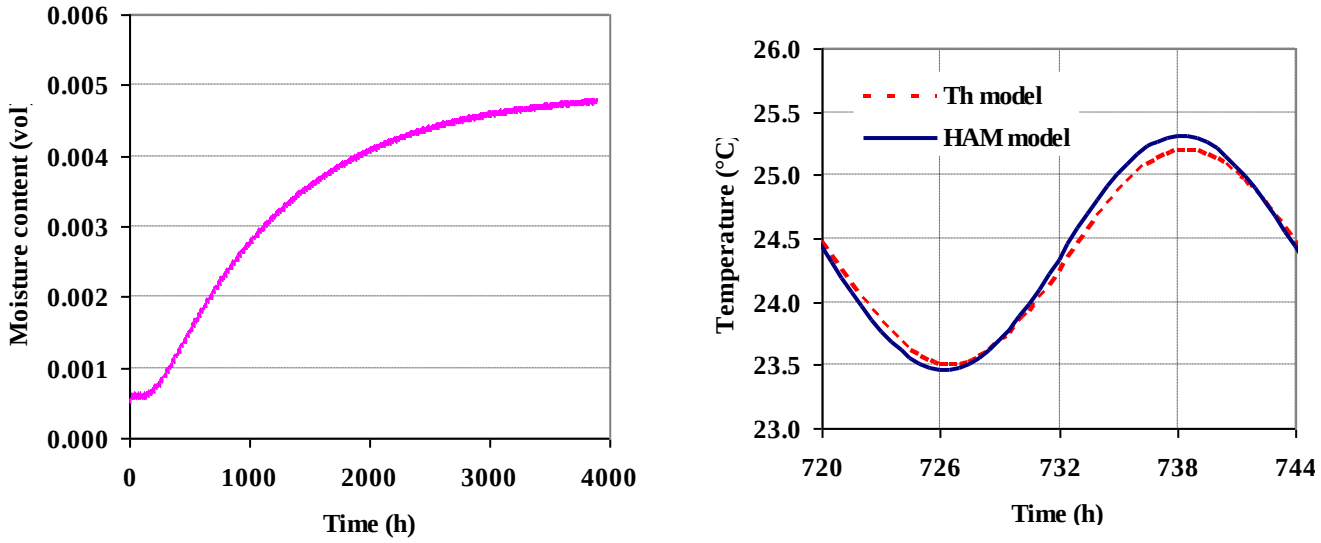

Fig. 10 : Time pattern of moisture content at 10 cm depth inside the brick wall and comparison between internal surface temperature for HAM and Th models after one month.

Hemp concrete wall

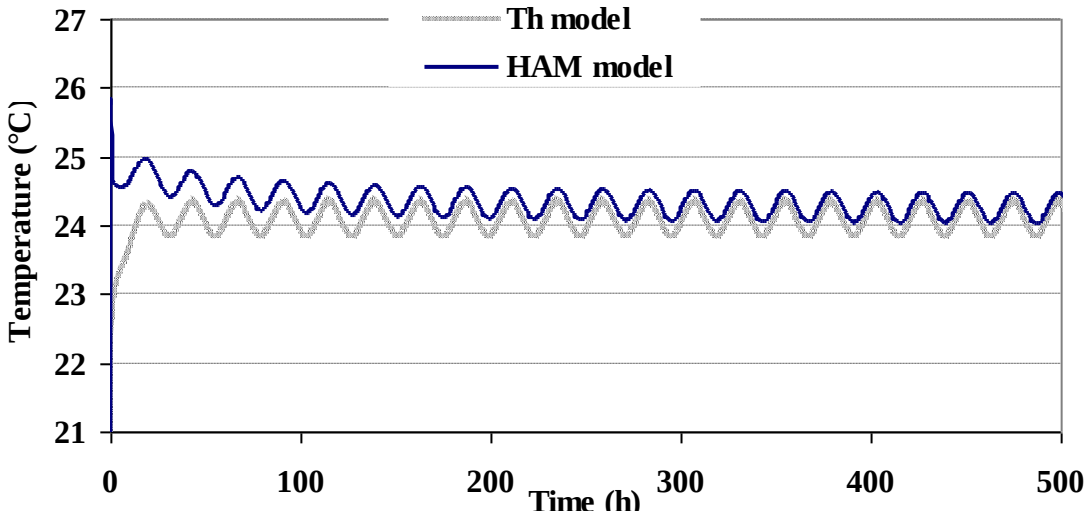

Fig. 11 : Comparison between internal surface temperature patterns for both Th and HAM models for the hemp concrete wall.

Taking into account moisture transfer through hemp concrete wall, leads to the variation of the thermal conductivity between 0.114 and 0.123 W/m K instead of 0.1058 W/m K for the Th model. Concerning the specific heat, its value vary between 1200 and 1350 J/kg °C instead of 1000 J/kg °C. In this case, the variation of volumic moisture content at 10 cm depth needs three monthes to reach small variations and thus internal surface temperature profile needs also three monthes to reach a steady variation.

Fig. 11 shows internal surface temperature profile for both HAM and Th models. In the first days the temperature of the HAM model is higher than that of the Th model because of the high adsorption of moisture through material pores. Then when moisture content tends to the equilibrium value, the difference between the two models becomes small. Because specific heat of moist material increases between 20 and 35%, temperature profile for the HAM model is expected to be more dampened and to have a higher time lag.

Fig. 12 shows internal surface temperature after one month and after three monthes for both Th and HAM model. After one month, the temperature varies between 23.99 and 24.43°C for the HAM model instead of 23.85 and 24.34°C for the Th model. So the amplitude of the HAM model is 0.22°C instead of 0.245°C. The time lag for the HAM model is also higher by thirty minutes. After 3 monthes, the temperature varies between 23.92°C and 24.34°C. Concerning the time lag it increases one hour.

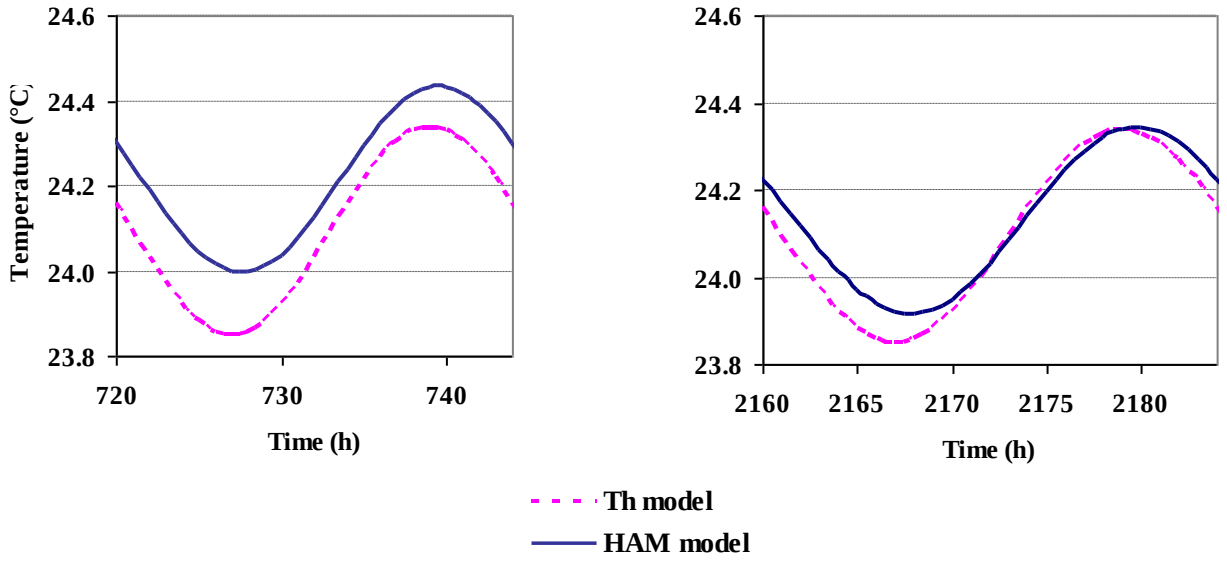

Fig. 12 : Comparison between the internal surface temperatures as computed by the Th and the HAM models after a period of one month and three monthes for the hemp concrete wall.

TABLE III:

COMPARISON BETWEEN TH AND HAM MODEL RESULTS FOR AFTER A PERIOD OF THREE MONTHES.

	Th model				HAM model (after 3 monthes)			
	Amplitude (°C)	Time lag (h)	Max. cond. flux (W/m^2)	Min. cond. flux (W/m^2)	Amplitude (°C)	Time lag (h)	Max. cond. flux (W/m^2)	Min. cond. flux (W/m^2)
Normal concrete	1.43	5.5	9.9	-4.42	1.36	5.5	9.8	-3.78
Brick	0.85	6.5	5.99	-2.5	0.94	6.25	6.63	-2.85
H. concrete	0.245	7	1.69	-0.75	0.21	8	1.73	-0.41

Table III compares Th and HAM models after three monthes and for the three materials. We can notice that taking into account moisture transfer has small impact on the time lag for brick and normal concrete walls. Concerning the amplitude of the internal surface temperature, while it increases about 10% in the brick wall, it decreases around 5% for the normal concrete. However for both walls it is expected to have more heat conduction entering from the outdoor space because of moisture adsorption as shown from the values of the conduction flux. Though the minimum heat flux decreases from -2.5 to -2.85 W/m^2 in the brick wall, its maximum value increases from 5.99 to 6.63 W/ m^2. For the concrete wall, while the maximum value decreases from 9.9 to 9.8 W/m^2, the minimum value passes from -4.42 to -3.78 W/ m^2 meaning that less heat would be extracted from the indoor space. For the hemp concrete wall, with the HAM model, the dynamic variation of the temperature is modified, its time lag is increased one hour and less heat is extracted from the indoor space. While the maximum conduction flux varies from 1.69 to 1.73 W/ m^2, the minimum value varies from -0.75 to -0.41 W/ m^2 which is 45% lower in absolute value! In the next sections we will study in details hemp concrete wall thermal inertia through studying effects of wall thickness, initial moisture content and material physical properties (sensitivity analysis).

C. *Effect of initial moisture content*

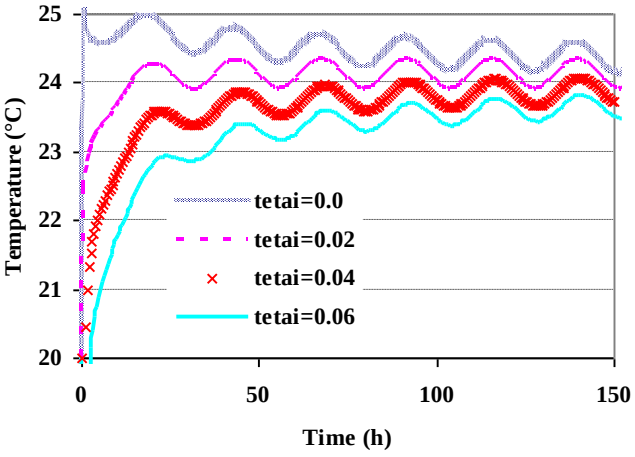

Fig. 13 : Time pattern of internal surface temperature of a 20 cm thickness hemp concrete wall for different initial volumic moisture content expressed in m^3/m^3.

Fig. 13 shows time pattern of internal surface temperature of a 20cm hemp concrete wall with initial volumic moisture content variating from 0 to 0.06 m^3/m^3. When the wall is initially dry its temperature is higher than other cases because of moisture adsorption phenomenon. As initial moisture content increases

temperature profile shifts down. For moist initial conditions as 0.06 m^3/m^3, the temperature profile is the lowest because of desorption phenomenon. One should note that for initial moisture conditions of 0.02 m^3/m^3 which is equilibrium moisture content at 50% of relative humidity, temperature profile is too close to that of the Th model for the first ten days.

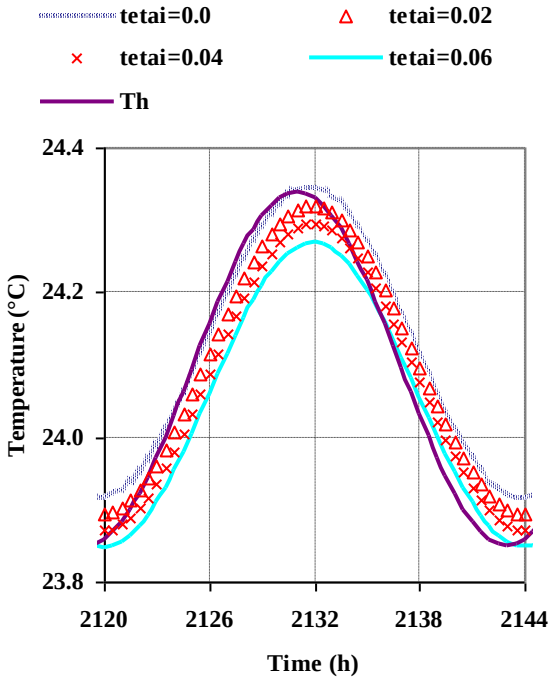

.

Fig. 14 : Comparison of internal surface temperature profile after three monthes for the Th and HAM model with different initial volumic moisture content expressed in m^3/m^3.

Fig. 14 shows time pattern of internal surface temperature after three monthes and for different initial moisture content conditions. As noted before, as initial moisture content is higher, temperature profile will be lower due to desorption. However the difference between these profiles decrease with time though it requires long periods for the equilibrium to be reached inside the material especially for high initial conditions. Concerning the Th case, temperature profile swings between the values of the maximum temperature of the dry initial conditions HAM model and the minimum temperature values of the wet initial conditions HAM model. These results show the importance of initial conditions on temperature profile. In the next section we consider initial conditions of 0.02 m^3/m^3 which is the closer to equilibrium conditions and we vary wall thickness.

D. Wall thickness

Table IV shows internal surface temperature amplitude and time lag for different hemp concrete wall thicknesses (from 5cm to 30cm) and for both Th and HAM models. It can be noticed that compared to the Th model, as wall thickness increases from 5 to 30 cm, amplitude of the HAM model is reduced from 7% to 19% and difference in time lag increases from 0.5 to 1.25 hours.

VI. Sensitivity Analysis

To better understand the influence of each parameter of the physical model on the results, a sensitivity analysis is done in this part. Fist, we analyse the impact of the specific heat capacity.

A. Specific heat capacity

Fig.15 and table V show the impact of the specific heat capacity on the internal surface temperature. A 25 % error of the specific heat has a significant impact on the time lag which is 6,5h; 8h and 9 h for the 0,75xCp; 1xCp and 1,25xCp cases respectively. Furthermore, when the specific heat capacity increases the amplitude of the internal surface temperature variation decreases because of the decrease of the thermal diffusivity. The amplitude variation for the reference case is 16% bigger than its 1,25xCp case by varying from 0.214 to 0.179°C.

TABLE IV :
COMPARISON OF TIME LAG AND TEMPERATURE AMPLITUDES FOR DIFFERENT WALL THICKNESSES AND FOR BOTH TH AND HAM MODELS

Thickness (cm)	5		10		15		20		30	
	Th	HAM	Th	HAM	Th	HAM	Th	HAM	Th	HAM
Amplitude(°C)	1.38	1.28	0.765	0.7	0.44	0.39	0.245	0.21	0.074	0.06
Time lag (h)	1	1.5	2.5	3	4.5	5.5	7	8	11.5	12.75

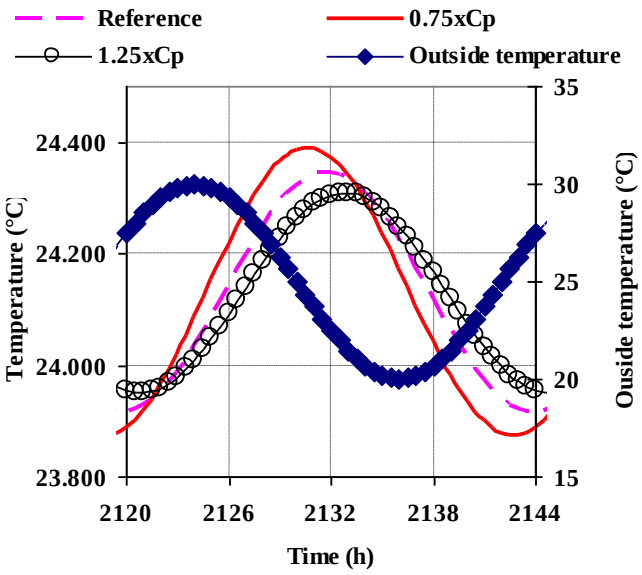

Fig. 15 : Impact of specific heat capacities on the internal surface temperature.

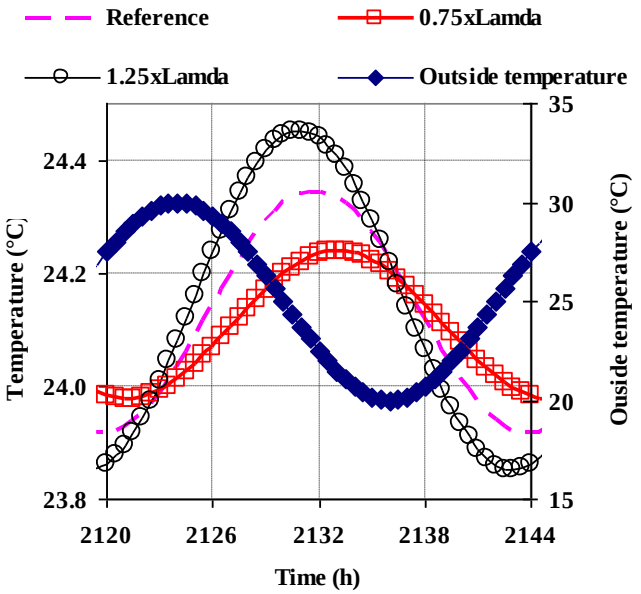

Fig. 16 : Impact of thermal conductivity on the internal surface temperature.

TABLE V:
IMPACT OF SPECIFIC HEAT CAPACITIES ON THE TIME LAG AND INTERNAL SURFACE TEMPERATURE

Internal surface temperature	Reference	0.75xCp	1.25xCp
Tmin (°C)	23.92	23.87	23.95
Tmax (°C)	24.34	24.39	24.31
Amplitude (°C)	0.21	0.26	0.18
Time lag (h)	8.0	6.5	9.0

TABLE VI:
IMPACT OF THERMAL CONDUCTIVITY ON THE TIME LAG AND INTERNAL SURFACE TEMPERATURE

Internal surface temperature	Reference	0.75xLamda	1.25xLamda
Tmin (°C)	23.92	23.99	23.86
Tmax (°C)	24.34	24.24	24.45
Amplitude (°C)	0.21	0.13	0.30
Time lag (h)	8	9	7

B. Mass density

The effect of the mass density on the internal surface temperature is identical as the case of specific heat capacities and is not plotted.

C. Thermal conductivity

The effect of the thermal conductivity on the internal surface temperature is shown in the table VI and the fig.16. As can bee seen in the fig 16, the thermal conductivity has a significant impact on the amplitude variation and the time lag. As the thermal conductivity increases, the thermal diffusivity increases. Therefore when increasing the thermal conductivity, the amplitude variation increases and the time lag decreases. For example when the thermal conductivity varies from 0.75xlamda to 1.25xlamda, the amplitude increases from 0.132 to 0.321 °C while the time lag decreases from 9 to 7 hours.

D. Sorption isotherm

Fig.17 and table VII show the influence of the sorption isotherm on the internal surface temperature. A ±25% error in the sorption isotherm has slight effect on the temperature. For both cases material relative humidity are too close, however for the 1.25xsorption material moisture content is higher, leading to a lower thermal diffusivity, so when the sorption isotherm varies from the 0.75xsorption case to the 1.25xsorption case, internal surface temperature varies from 0.23 to 0.2°C and time lag increases from 7.5 to 8.2 h.

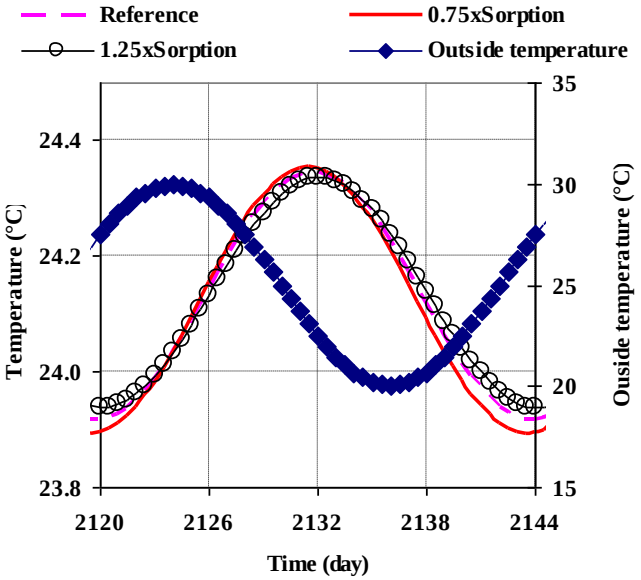

Fig. 17 : Impact of the sorption isotherm on the internal surface temperature.

TABLE VII :
IMPACT OF SORPTION ISOTHERM ON THE TIME LAG AND INTERNAL SURFACE TEMPERATURE

Internal surface temperature	Reference	0.75xSorption	1.25xSorption
Tmin (°C)	23.92	23.89	23.94
Tmax (°C)	24.34	24.35	24.34
Amplitude (°C)	0.21	0.23	0.20
Time lag (h)	8.0	7.5	8.2

E. Transport coefficients $D_{T,v}$, D_T

The transport coefficients $D_{T,v}$ and D_T have a very small effect on the internal surface temperature and they are not plotted here.

F. Transport coefficient D_θ

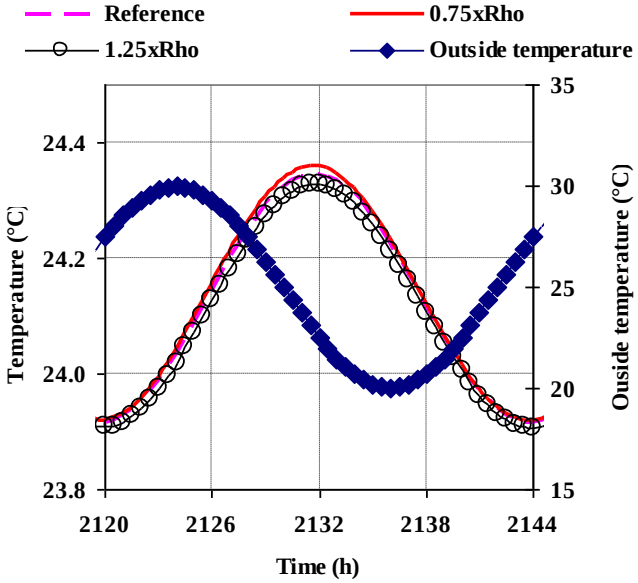

Fig. 18 : Impact of the transport coefficient associated to a moisture content gradient on the internal surface temperature.

TABLE VIII :
IMPACT OF TRANSPORT COEFICIENT D_θ ON THE TIME LAG AND INTERNAL SURFACE TEMPERATURE

Internal surface temperature	Reference	0.75xDteta	1.25xDteta
Tmin (°C)	23.92	23.92	23.91
Tmax (°C)	24.34	24.36	24.33
Amplitude (°C)	0.214	0.22	0.21
Time lag (h)	8.0	8.0	8.0

One can see in Fig.18 that the transport coefficient D_θ has a slight effect on the internal surface temperature. When D_θ decreases about 25%, temperature amplitude increases about 0.006°C which is about 2.5% and there are no differences in time lag. It can be seen also that decreasing the transport coefficient D_θ leads to an increase in the maximum internal surface temperature because of decreasing of the water vapour desorption quantity in the internal surface wall.

G. External heat and mass convection coefficients surface

The simulation results show that the impact of external heat and mass convection coefficients on the internal surface temperature is negligible and is note depicted here.

H. Internal heat and mass convection coefficients

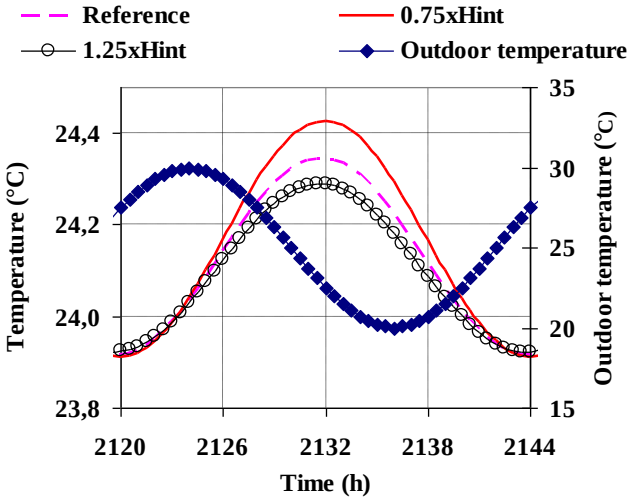

Fig. 19 : Impact of the heat and mass convection coefficients of internal surface on the internal surface temperature.

Fig.19 and table IX show the impact of the internal heat and mass convection coefficients on the internal surface temperature. As the convection coefficients are higher, temperature profile will tend to the indoor temperature and thus it will be decrease due to heat loss from internal surface to indoor ambiance. The amplitude of temperature variation decreases 14.5% when the heat and mass convection coefficients at internal surface increase 25%. Furthermore, concerning the time lag, it varies from 7.5 to 8.2 hours when the heat and mass convection coefficients vary from 1.25xHint to 0.75xHint respectively.

TABLE IX :
IMPACT OF HEAT AND MASS CONVECTION COEFICIENTS OF THE INTERNAL SURFACE ON THE TIME LAG AND INTERNAL SURFACE TEMPERATURE

Internal surface temperature	Reference	0.75xHint	1.25xHint
Tmin (°C)	23.915	23.91	23.92
Tmax (°C)	24.34	24.43	24.29
Amplitude (°C)	0.21	0.258	0.183
Time lag (h)	8.0	8.2	7.5

VII. SIMULATION UNDER OUTDOOR REAL CONITIONS

In the previous sections we studied the behaviour of a simple hemp concrete wall under outdoor periodic temperature and relative humidity. However, in reel conditions, the wall is exposed to non periodical variations and to solar radiation which is taken into account in the boundary condition of equation (6). To investigate wall behaviour under reel

conditions, we run simulations for a 20 cm hemp concrete vertical wall facing West and under summer conditions of Carpentras and Ajaccio cities in South France (Fig. 20). Carpentras has a hot dry climate with high temperature difference between day and night (temperature varies between 15 and 35°C and relative humidity between 80% and 40% respectively). Ajaccio has a softer temperature but more humid weather (temperature between 15 and 30°C and relative humidity between 95% and 50% respectively). Simulations were run for both Th and HAM models and for external solar radiation absorption coefficient variating from 0.2 (light color surface) to 0.8 (dark color).

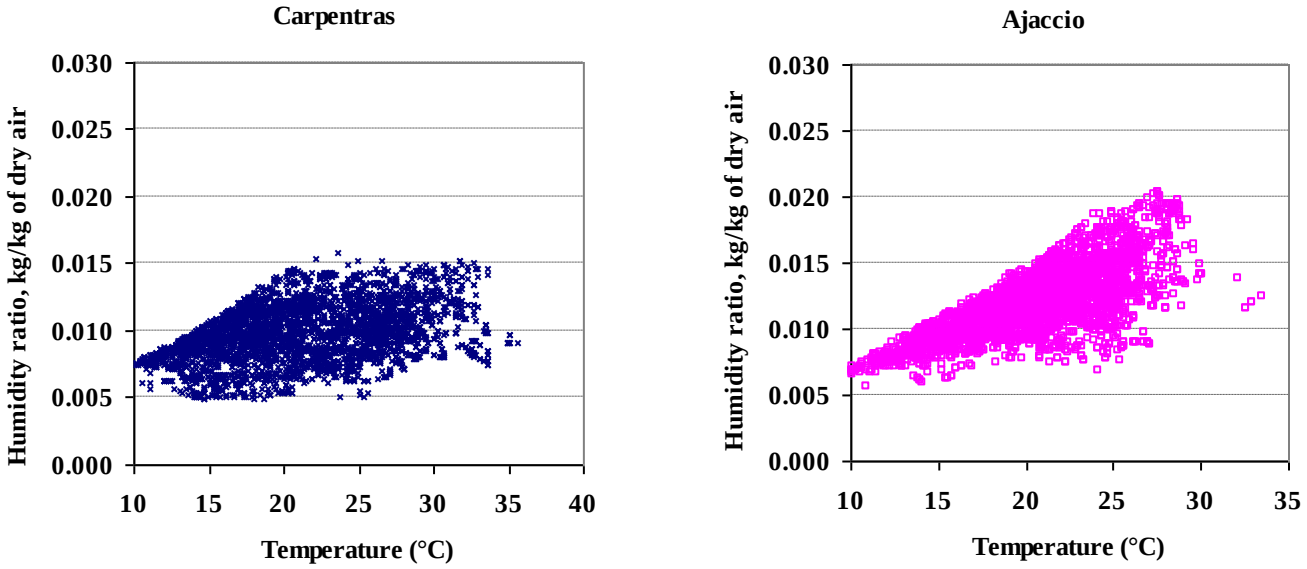

Figure 20: Climatic conditions for Carpentras and Ajaccio cities.

A *Results*

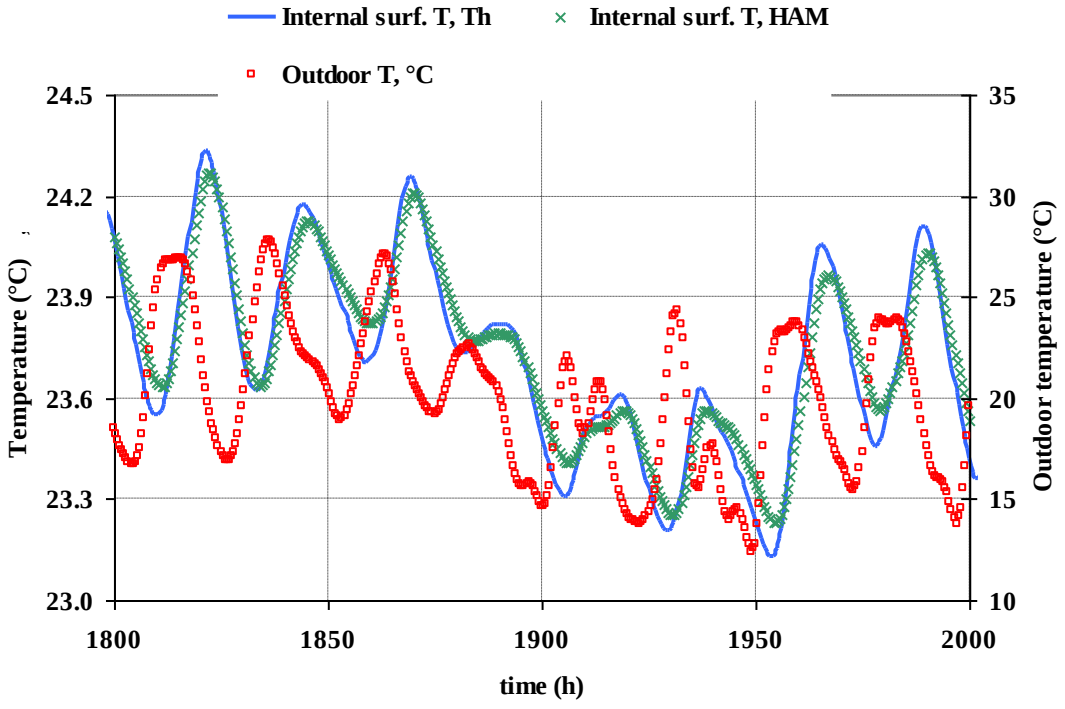

Fig. 21: Comparison of internal surface temperature time patterns of both Th and HAM models for Ajaccio conditions (α=0.6).

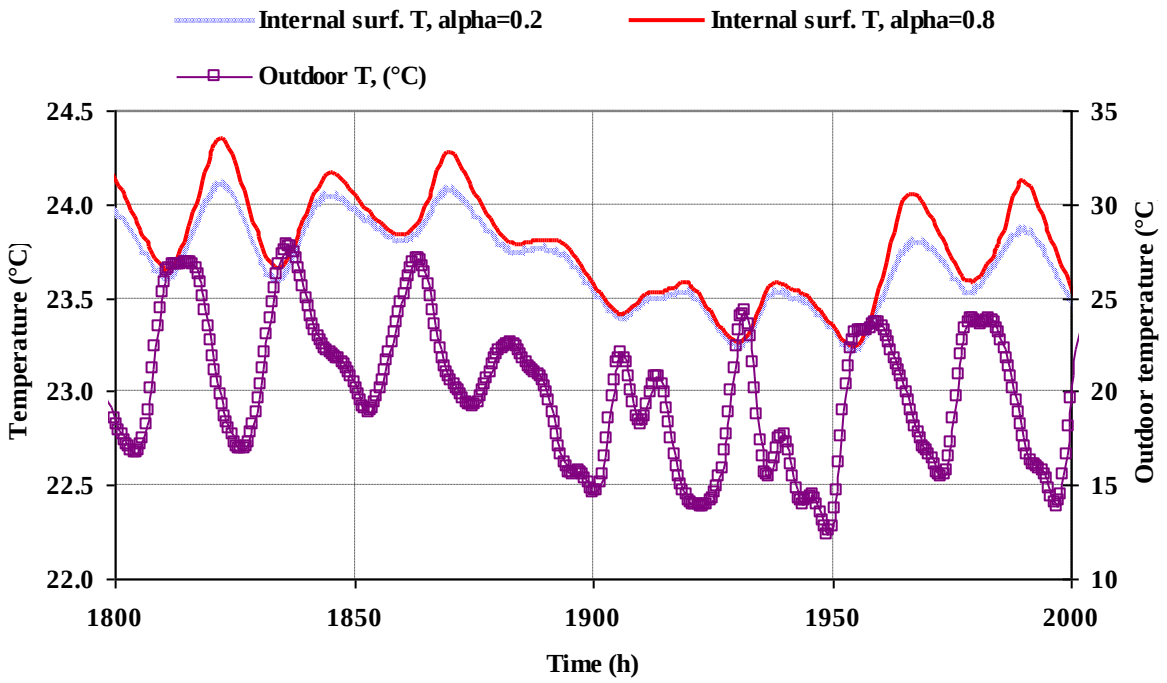

Fig. 22: Internal surface temperature time patterns for the HAM model and for values of absorption coefficient of 0.2 and 0.8.

Fig. 21 shows internal surface temperature for both Th and HAM models for Ajaccio conditions for a week in summer. It can be seen that its amplitude varies around 0.5°C because outdoor solar radiation is taken into account. Comparing HAM and Th models, we notice that HAM model temperature is more dampened and shifted than Th model temperature. Differences can reach 0.15°C and 1h in amplitude and time lag respectively.

Fig. 22 shows internal surface temperature variation for the HAM model when external solar radiation absorption coefficient varies from 0.2 to 0.8. As absorption coefficient increases from 0.2 to 0.8, internal surface temperature variation can reach 0.35°C. It can be noticed that during night when there are no solar radiation, temperatures of both cases are too close and during cloudy days also there are very slight difference between both models (Fig. 21, time 1900-1950 h).

Concerning Carpentras conditions, the same remarks apply also. However because outdoor weather is hotter, internal surface temperature amplitude is bigger around 0.8°C and the difference between Th and HAM models is around 0.2°C in amplitude and 1h in time lag. The difference is more accentuated than for Ajaccio conditions because internal surface temperature variation is higher with the same internal relative humidity which means that desorption rate is higher (in both cases moisture transfer occurs from the outdoor surface toward indoor surface). Besides when absorption coefficient varies from 0.2 to 0.8; internal surface temperature can increase about 1°C.

Fig. 23 shows wall conduction heat loads as a function of solar radiation absorption coefficient for both HAM and Th models and for Carpentras and Ajaccio cities. These are computed from the calculation of convection flux between internal wall surface and indoor temperature (taking into account the cases where only internal surface temperature is higher than indoor temperature). It can be seen that these loads are higher for Carpentras and they increase when absorption coefficient increases. For both cases, Th model results are higher because internal surface temperature is less dampened.

The difference between both models results varies from 10% to 8% when absorption coefficient varies from 0.2 to 0.8 in Ajaccio and from 18% to 6% in Carpentras. The difference in % tends to decrease as the absorption coefficient increases because the amount of sensible heat absorbed (solar radiation) increases especially for Carpentras which suggests that thermal inertia is less sensitive to moisture transfer for high solar absorption coefficients in hot dry regions (less sensitive but it still cannot be neglected in hemp concrete walls).

VIII. Conclusion And Perspectives

In this paper, we have studied the effect of moisture transfer on thermal inertia of simple layer walls. Internal surface temperature amplitude and time lag were computed under summer periodical variating conditions and for three materials: normal concrete, brick and a vegetal fiber material: hemp concrete. Our results suggest that under normal humidity conditions, neglecting moisture transfer has small impact on the thermal performance of brick walls, may lead to overestimate indoor extracted heat in normal concrete walls and has a great impact on the thermal behaviour of hemp concrete walls especially as thickness increases. Besides, for the hemp concrete wall, effect of wall thickness and initial moisture content were investigated. It was shown that results depend strongly on initial moisture content and it needs several monthes to decrease initial conditions effect. Furthermore, a sensitivity analysis of internal

surface temperature to different physical parameters has been done. Our results suggest that the internal surface temperature is very sensitive to the thermal properties, sorption isotherm; transport coefficient associated to moisture gradient and to the internal heat and mass convection coefficients. Finally simulations under real climatic conditions showed that, depending on external solar radiation coefficient value, neglecting moisture transfer can lead to important differences in envelope conduction loads (between 18 and 6%).

However these results were obtained neglecting hysteresis effect in the sorption curve which could be non negligible especially in hemp concrete walls. Moisture transport coefficients were assumed constant which could also affect moisture distribution. So these cases should be studied carefully.

The impact of moisture transfer should also be computed on the whole building level.

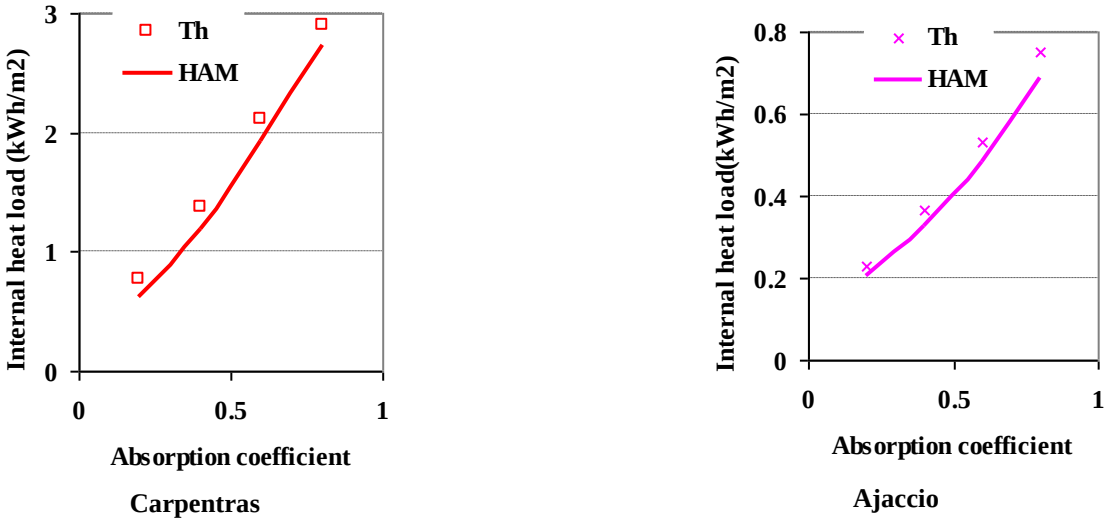

Figure 23: Internal heat conduction loads as function of solar radiation absorption coefficient for both Th and HAM models and for Carpentras and Ajaccio cities

REFERENCES

[1] J.L. Cnaletti, G. Notton, A. Damian, I. Colda, C. Cristofari."New concept of solar air heater integrated in the building". *4th IASME/WSEAS International Conference on Energy, Environment, Ecosystems and Sustainable Development*, Algarve, Portugal, pp. 52-59, 2008.

[2] C. Maalouf, A.D. Tran Le, L. Chahwane, M. Lachi, E. Wurtz, T.H. Mai – "A study of the use of thermal inertia in simple layer walls and its application to the use of a vegetal fiber material in buildings", *International Journal of Energy, Environment and Economics*, to be published.

[3] P.T. Tsilingiris,"Thermal flywheel effects on the time varying conduction heat transfer structural walls", *Energy and Buildings*, Volume 35, Issue 10, pp. 1037-1047, 2003.

[4] H. Asan, Y.S. Sancaktar, "Effects of Wall's thermophysical properties on time lag and decrement factor", *Energy and Buildings*, 28, pp.159-166, 1998.

[5] R.J. Duffin, G. Knowles,"A passive wall design to minimise building temperature swings", *Solar Energy* 33 (3/4) 337-342, 1984.

[6] T.D. Xenos."Sustainable masonry building-shell design of byzantine monuments in Greece for energy efficient constructions*", Proceedings of the 2006 IASME/WSEAS International Conference on Energy & Environmental Systems*, Chalkida, Greece, May, pp. 68-75; 2006.

[7] H. Altan, "Windows and building envelopes, and their influence on indoor thermal comfort". *Proceedings of the 4th IASME/WSEAS International Conference on Energy & Environment*, Cambridge, pp. 259-262, 2009.

[8] S. Bica, L. Roşiu, R. Radoslav."What characteristics define ecological building materials"; *Proceedings of the 7th IASME/WSEAS International Conference on Heat Transfer Thermal Engineering & Environment*, Moscow, pp. 159-164. 2009.

[9] E.F. Sowell, P. Haves. "Efficient solution strategies for building energy system simulation", *Energy and Buildings*, vol. 33, p. 309-317, 2001.

[10] C. Maalouf, E. Wurtz, L. Mora, "Effect of Free Cooling on the Operation of a Desiccant Evaporative Cooling System", *International Journal of Ventilation*, vol. 7, pp. 125-138, 2008.

[11] E. Wurtz , F. Haghighat , L. Mora, K.C. Mendonca, C. Maalouf, H. Zhao, P. Bourdoukan, "An integrated zonal model to predict transient indoor humidity distribution", *ASHRAE Transactions*, (112) 2, pp. 175-186, 2006.

[12] Mora L, Wurtz E, Mendonça K.C, Inard C. "Effects of coupled heat and moisture transfers through walls upon indoor environment predictions", *International Journal of Ventilation;* 3(3): 227 – 234, 2004.

[13] J.R. Philip and D.D. De Vries, "Moisture movement in porous materials under temperature gradients", *Transaction of American Geophysical Union.* V.38, n.2, p.222-232, 1957.

[14] C.R. Pedersen., "Prediction of moisture transfer in building constructions", *Building and Environment* (3) 387–397, 1992.

[15] M. Kunzel, "Simultaneous heat and moisture transport in building components", Fraunhofer Institute of building physics, Germany, 1995, http://www.wufi.de/index_e.html (section: Literatur).

[16] N. Mendes, " Models for prediction of heat and moisture transfer through porous building element", PhD, Federal University of Santa Catarina, Florianopolis, SC, Brésil, p. 225.

[17] A.D. Tran le, C. Maalouf, K.C. Mendonça, T.H. Mai, E. Wurtz, " Study of moisture transfer in doubled-layered wall with imperfect thermal and hydraulic contact resistances", *Journal of Building Performance Simulation*; 2: 251-266, 2009.

[18] Annex 41, "Collection of reports of common exercise 1: Case 0A & Case 0B", International Energy Agency, Annex 41 – Subtask, vol.1, 2005.

[19] T. Terashima and M. Mizuhata, "Moisture movement in double layer building materials".*Proceedings of Clima 2000 Conference*.

[20] A.D. Tran Le, C. Maalouf, T.H. Mai, E. Wurtz, F. Collet, "Transient hygrothermal behaviour of a hemp concrete building envelope", Energy and Buildings, DOI: 10.1016/j.enbuild.2010.05.016 (2010).

[21] WUFI, Wärme und Feuchte instationär: http://www.wufi.de/index_e.html (section: Basics, Moisture Storage Function).

[22] V. Cerezo, "Propriétés mécaniques, thermiques et acoustiques d'un matériau à base de particules végétales : approche expérimentale et modélisation théorique", PhD, INSA & ENTPE de Lyon, p. 242, 2005.
[23] F. Collet, "Caractérisation hydrique et thermique de matériaux de génie civil à faibles impacts environnementaux, *PhD*, INSA de Rennes, p. 220 , 2004.